# Spatiotemporal resonances in a microfluidic system

A. Dodge,[1] A. Hountondji,[1] M. C. Jullien,[2] and P. Tabeling[1]
[1]*Microfluidics, MEMS, Nanostructures, ESPCI, 10 rue Vauquelin, 75231 Paris, France*
[2]*SATIE, ENS-Cachan, Campus de Ker Lann, 35170 Bruz, France*
(Received 7 February 2005; published 9 November 2005)

We report on the experimental observation of a spatiotemporal resonance phenomenon, in which a temporal excitation locks with a spatial pattern in an open flow system. The observation is made in a microfluidic system. We obtain the expected regimes—mixing and resonant patterns—in qualitative agreement with the theory. As an application, we realized a dual system particle extraction–micromixer.

DOI: 10.1103/PhysRevE.72.056312 PACS number(s): 47.52.+j, 47.54.+r

## I. INTRODUCTION

Since the early days of microfluidics, it was recognized that miniaturization, by imposing flows to be laminar, considerably facilitates the handling of liquids in microsystems. Most of the microdevices made in the last ten years took advantage of this capability (see recent reviews, Refs. [1–3]). Several fluidic manipulations, standing well beyond the reach of ordinary hydrodynamic systems, have thus been demonstrated. For instance, it has been shown that 30-nm-thin stable liquid streams can be reliably obtained in microchannels [4], that tunable chemical gradients can be created [5], and that different fluids can be driven through mazes of microchannels under full control, and without being disturbed by turbulent perturbations [6]. All these contributions demonstrated interesting fluidic capabilities that are often inaccessible to nonminiaturized hydrodynamics. The objective of the present work is to make progress in the same direction by producing, under full control, interface patterns of variable shapes, and exploit them to achieve tasks of practical interest. The present work qualitatively confirms a recently published theoretical work [7], which predicted that mixing can be achieved in a cross-channel intersection, under certain conditions, but that also, if "resonance" conditions are satisfied, reversible stretching of the interface is obtained. The present paper fully demonstrates the two effects, and exploits them to realize a microdevice that is based on a simple geometry, and is able to both mix or extract.

## II. PRINCIPLE OF THE EXPERIMENT

The dynamical effect we address here takes place in a geometry shown in Fig. 1. The system is based on a cross-channel micromixer geometry [8–11]. In this geometry, a pair of fluids flows side by side, in a channel, then passes through an intersection [see Fig. 1(a)]. At the intersection, a time-dependent flow coming from the sides is superimposed with the main stream. This additional flow perturbs the shape of the interface between the two fluids to different extents depending on the amplitude and frequency of the side flow. Typically, when the perturbation amplitude is small, or its frequency large, weak oscillations are generated at the interface between the pair of fluids forming the mean stream [Fig. 1(b)]. When the amplitude is large, and the frequency moderate, stretching and folding of the interface is produced [Fig. 1(a)]. In such regimes, the interface between the pair of fluids is highly circonvoluted and thus mixing is favored [12]. In the system we consider, resonance conditions also exist,

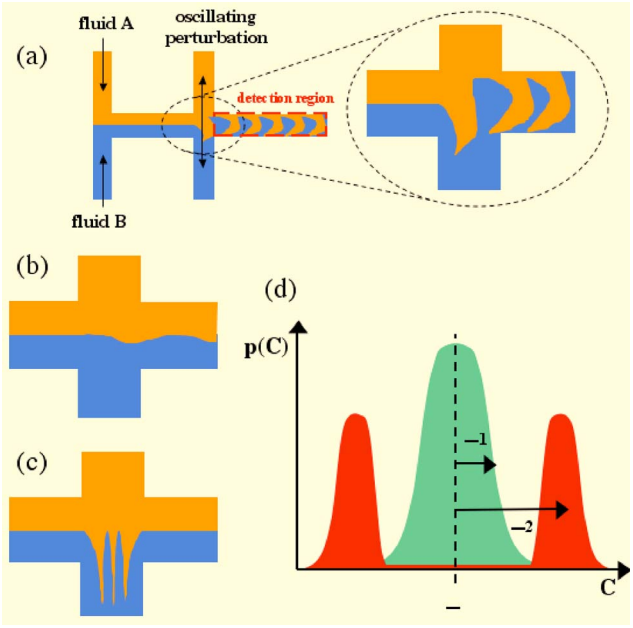


FIG. 1. (Color online) Sketch of the system: two miscible fluids (A and B) flow, side by side, towards a cross-channel intersection. At the intersection, an additional, time-dependent side flow is driven. When the perturbation amplitude is small, or its frequency large, weak oscillations are generated at the interface between the pair of fluids forming the mean stream (b). When the amplitude is large, and the frequency moderate, stretching and folding of the interface is produced [see (a)]. In such regimes, the interface between the pair of fluids is highly circonvoluted and mixing takes place. Resonance conditions also exist, for which the interface is strongly distorted in the active region, but returns to a flat shape afterwards [see (c)]. Plot (d) represents two typical distributions for the concentration field of a tracer labeling one of the two fluids, A or B: a well-mixed regime, such as (a), gives rise to the distribution, which is narrowly centered around an averaged value, while regimes (b) and (c) give rise to bimodal distributions. The variances are typically small in the well mixed regime, and (comparatively) large in the bimodal cases. Measuring the variance of the concentration distributions is thus a way to discriminate different cases.

 

for which the interface is strongly distorted in the active region, but returns to a flat shape afterwards [Fig. 1(b)]. This situation arises when the traveling time of the fluid particles through the active zone is equal to an integer number times the oscillating period [7]. This effect is a different dynamical phenomenon, involving a particular interaction between space and time. It is interesting to mention at this stage the work of Niu and Lee [12] who studied an infinitely replicated cross-channel intersection, and analyzed it in the framework of dynamical systems theory [12]. Their work may suggest that the resonant states and the circonvoluted patterns of the single unit are reminiscent, respectively, of Kolmogorov-Arnold-Moser (KAM) trajectories and chaotic states of the infinitely replicated system [13].

One may characterize the different patterns existing within the system by introducing the following quantity:

$$\sigma^2 = \langle [C(\mathbf{x},\mathbf{t}) - \mu]^2 \rangle.$$

Here, the brackets mean averaging in space over the whole channel width, and a fixed channel length beyond the intersection, and in time over a period of the forcing. In practice, in the experiment, the channel length we will be using is 2 mm. In the above expression, $C(\mathbf{x},\mathbf{t})$ is the concentration of a tracer labeling one of the two fluids [either A or B in Fig. 1(a)], $\mu$ is the mean value of $C(\mathbf{x},\mathbf{t})$ (constant for all regimes due to conservation of material). $\sigma^2$ is thus the variance of the concentration field, averaged in time. Figure 1(d) represents, schematically, typical concentration distributions for two different regimes: a well mixed regime will have a concentration distribution closely centered around the mean value $\mu$ and therefore a small variance ($\sigma_1^2$). A nonmixed regime, corresponding to weak perturbations or resonant patterns, will have a bimodal distribution and, consequently, a substantial variance ($\sigma_2^2$). Measuring the variance of the concentration distributions is thus a way to discriminate different cases. The experimental observation and characterization of the different regimes, along with their use for producing interesting functionalities, is the subject of the present paper.

## III. EXPERIMENTAL SETUP

Our experimental system is shown in Fig. 2. It consists of a main channel where two streams of glycerol flow side by side, one flow being marked with fluorescein and the other unmarked. A series of ten integrated PDMS valves are disposed in a comb-shaped fashion onto the two channel branches perpendicular to the main flow. These valves are made using multilayer soft lithography (abbreviated as MSL) [13]. The valves consist of actuation channels, filled with water; these channels compress a membrane, closing or opening a segment of the microfluidic channel, depending on the pressure applied to them. As the comb-configured valves close on one branch—in a peristaltic fashion—they create a displacement of fluid at the channel intersection located at the center of the device. Releasing the pressure applied to one comb and applying pressure on the other comb creates a flow in the opposite direction. Therefore it is possible to create an oscillating flow with a specific frequency and amplitude at the cross-channel intersection. The displacement

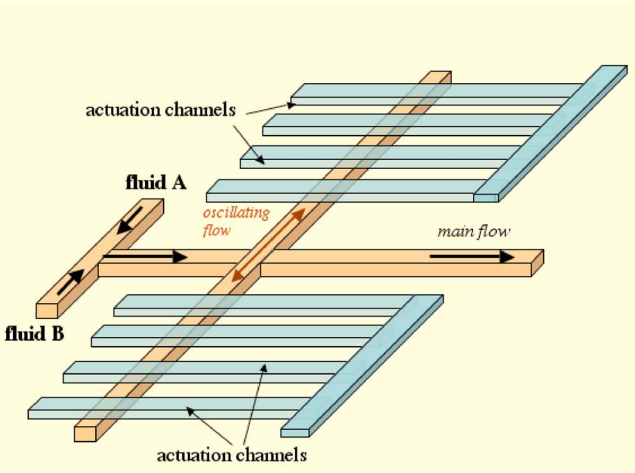


FIG. 2. (Color online) Sketch of the experimental system used in the report: the fluids A and B are driven by a syringe pump, ensuring the same flow rate for the two fluids. The interface between them is perturbed by an oscillating flow produced by the periodic closing and opening of PDMS valves which are made by using MSL technology. A homemade electronic circuit driving two LEE valves controls the arrival of an in-house network of compressed air line which pushes DI water located in the actuation channels. A function generator controls the frequency at which the LEE valves are switched on and off, thereby setting the lateral perturbation frequency. A Cohu charge-coupled device camera mounted onto a Leica Binocular MZFL III was used to acquire images of the fluorescent patterns created in the microfluidic channels. The dimensions of the channels are 23 $\mu$m high, and 200 $\mu$m wide; the main channel is 20 mm long.

amplitude is related to the pressure applied to the actuation channels. The frequency is that imposed by the system monitoring the electrovalves. The flow is visualized by using epifluorescence microscopy; the video images are recorded and processed by using MATHLAB™ software. We checked that the intensity is proportional to the dye concentration for the range of concentrations we considered. The method averages out the concentration profiles across the channel depth, and thus does not resolve its three-dimensional (3D) spatial structure. We will comment on this point in the discussion of the results.

## IV. EXPERIMENTAL RESULTS

We investigated up to 500 different experimental conditions, keeping the flow rate fixed, and varying the actuation frequencies $f$ and pressures $P$ of the valves between 0.5 and 5 Hz, and 0.2 and 1.4 bars, respectively. We systematically measured the averaged variance of the concentration field $\sigma^2$ (introduced above) to characterize the various flow patterns. The isoplot of $\sigma^2$ is displayed in Fig. 3. At large frequencies, the interface is weakly perturbed [see Fig. 3(b)]; in such a case, the concentration field is stepwise, and the probability distribution function of the concentration field in the spatiotemporal frame defined above is bimodal. This situation corresponds to the largest variances $\sigma^2$ we obtained. In the mixed regimes, such as the one shown in Fig. 3(a), the con-

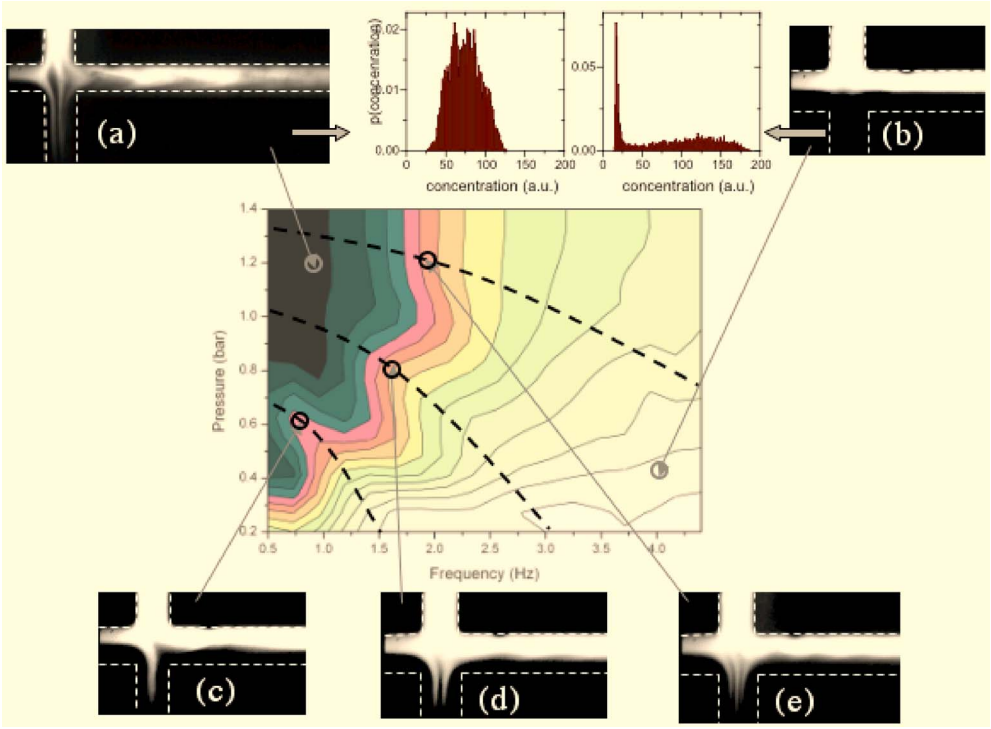


FIG. 3. (Color online) Regimes observed for different actuation pressure and frequencies of the oscillating pump, acting on the side channels. The pressure-frequency diagram is established for a fixed flow rate, in the main channel, equal to 0.04 $\mu$L/min. The diagram represents the isolines of the variance $\sigma^2$ defined in the text. The scale of $\sigma^2$ levels decreases linearly from white ($\sigma^2$=3000) to black ($\sigma^2$=240). At small $\sigma^2$ one has mixing regimes, illustrated in (a). At large $\sigma^2$ (white area) we have weakly perturbed regimes, illustrated in (b). We display the concentration distributions of fluorescein, found experimentally for these two cases. The resonance regimes—i.e., those for which the interface is strongly distorted in the intersection, but returns straight again after the intersection—are illustrated in (c), (d), and (e). Resonance regimes can be classified according to the number of tendrils appearing in the intersection. One can see (c) one tendril, (d) two tendrils, (e) three tendrils. The dashed lines uncover the ensemble of the resonance conditions, as found experimentally. The detailed experimental parameters for (a)–(e) are the following: (a) $f$=0.7 Hz, $P$=1.2 bars; (b) $f$=4.0 Hz, $P$=0.4 bar; (c) $f$=0.8 Hz, $P$=0.6 bar; (d) $f$=1.7 Hz, $P$=0.8 bar; (e) $f$=2.2 Hz, $P$=1.3 bars. Fluorescein concentration is 0.3 mM. Glycerol solution concentration is 80%.

centration distribution peaks around an averaged value, and $\sigma^2$ is smaller. Note that the term "mixed" refers to the concentration field averaged across the channel height. It is not ascertained that the system is mixed across the channel. We have not investigated this issue here; we will keep the term "mixed" for simplicity.

The boundaries between the "mixed" and unmixed regimes develop tongues as in the theoretical diagram of Ref. [7]. The resonance phenomenon takes place along the dotted lines in Fig. 3. As is shown by the theory, the order of the resonance is indicated by the number of tendrils appearing in the intersection. We were able to observe up to three tendrils, corresponding to the "third" resonance ($n$=3) in the terminology of Ref. [7]. The corresponding flow patterns are displayed in Figs. 3(c)–3(e).

We may underline here the excellent qualitative agreement with our observations and the theoretical and numerical work of Ref. [7]: the agreement concerns the patterns obtained at the resonances (strikingly similar to those of Fig. 2 of Ref. [7]) and the overall shape of the phase diagram (similar to Fig. 4 of Ref. [7]).

In resonant conditions, the interface is temporarily and reversibly stretched as it goes through the intersection, and eventually regains a straight shape. This phenomenon can be used to devise a fully controlled mixer-extractor, as shown in Fig. 4. In order to demonstrate this effect, we added both fluorescent microbeads, of 1 $\mu$m in diameter, and fluorescein to the upper fluid layer (a mixture of 50% glycerol and water). The lower layer consists of the glycerol-water mixture only. The extraction we perform is based on the existence of a contrast between the diffusion constants of two sets of particles, a mechanism similar to the so-called H filter [14,15], a microdevice which extracts smaller molecules from larger ones in solution. In our case, the first set of particles is the fluorescein molecules, and the second set is the fluorescent beads. The diffusion constant of the former is three orders of magnitude greater than the latter. Figure 4 shows the system operating in different regimes. When no actuation is imposed, a sharp and flat interface between the lower and upper fluid layers is visible beyond the active zone [Fig. 4(a)]; this shows that fluorescein molecules and beads remain in the upper part of the main channel. This is an expected result, considering the low values of the diffusion coefficients at hand. In the circonvoluted regimes, fluorescein molecules and beads are mixed thoroughly after passing the intersection [Fig. 4(c)]. In the resonant regimes, and well within the folds of the isolines of Fig. 2, the interface is strongly elongated and folded during the time it crosses the

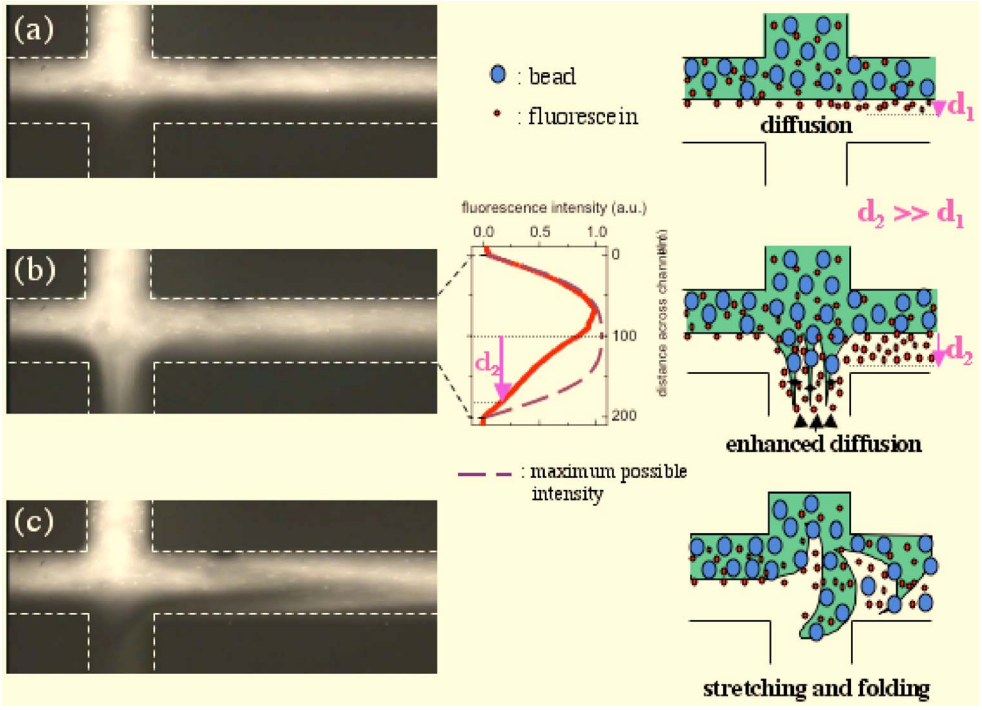


FIG. 4. (Color online) Controlled extraction and mixing on the same chip: (a) no actuation; particles are simply transported from the left to the right. (b) Resonant regime with three tendrils: the smaller particles diffuse more rapidly across the interface than the larger ones. This effect is enhanced by the temporary strong gradients taking place in the active zone when resonance occurs. All the fluorescent beads remain in the upper channel region. (c) Mixing: the particles are mixed thoroughly. Experimental conditions in the three conditions: glycerol solution concentration is 50%. Fluorescein concentration is 0.3 mM. Fluorescent beads are at a concentration of $10^8$ beads/mL. Flow rate in the main channel is 0.1 $\mu$L/min. (d) Concerntation profiles obtained respectively without actuation (full line) and in a resonant regime (dashed line).

intersection, but returns to a flat shape upon leaving the intersection. As a consequence, while the interface is in the active zone, developing tendrils, the characteristic scale of the concentration field shrinks and the diffusion processes across the interface are enhanced. In our experiment, we observed that the fluorescein has invaded the channel after passing through the active zone, while the beads remain localized on their original side of the channel [see Figs. 4(b)–4(d)]. The profiles of Fig. 4(d) show that fluorescent material has diffused in the lower part of the channel when the system operates in the resonance regime while Fig. 4(b) indicates that in the same conditions all beads remain on the same side. These observations thus show that fluorescein has been successfully extracted from the initially homogeneous mixture. For the range of experimental conditions we investigated, the extraction reaches a maximum level at a frequency of 1 Hz. At this maximum, the quantity of fluorescein we could extract was 30% of the amount initially present in the upper layer. The "resonant" extractor we report here operates like the H filter [14], but with a much higher efficiency: to obtain the same result with an H filter would require a channel length one hundred times larger than the one we have used here.

## V. CONCLUSION

To conclude, we observed in this experiment an interesting phenomenon, in which spatial patterns and temporal excitation lock in, in an open flow. Our work confirms—albeit at a qualitative level—the theoretical expectations. We finally used this knowledge to make co-exist, within the same device, both mixing and extraction.

## ACKNOWLEDGMENTS

The authors thank Centre National de la Recherche Scientifique, Ecole Supérieure de Physique et Chimie de Paris, and EEC (under Grant No. HPRN-CT-2002-00300) for their support to this research. They have benefitted from instructive discussions with S. Niu and Y. K. Lee. We thank J. B. Salmon for his help in the image processing, and S. Chen, for her editorial help.

[1] H. A. Stone, A. D. Stroock, and A. Ajdari, Annu. Rev. Fluid Mech. **36**, 381 (2001).
[2] D. Reyes, D. Iossifidis, P-A. Auroux, and A. Manz, Anal. Chem. **74**, 2623 (2002); P. A. Auroux, D. Iossifids, D. Reyes, and A. Manz, *ibid.* **74**, 2637 (2002).
[3] P. Tabeling, *Une Introductionà la Microfluidique*, Eds Belin (2003).
[4] J. Knight, A. Vishwanath, J. Brody, and R. Austin, Phys. Rev. Lett. **80**, 3863 (1998).
[5] N. L. Jeon, H. Baskaran, S. K. Dertinger, G. M. Whitesides, L. Van de Water, and M. Toner, Nat. Biotechnol. **20**, 826 (2002).
[6] T. Thorsen, S. Marrkl, and S. Quake, Science **298**, 580 (2002).
[7] F. Okkels and P. Tabeling, Phys. Rev. Lett. **92**, 038301 (2004).
[8] Y. K. Lee, C. Shih, P. Tabeling, and C. M. Ho (unpublished).
[9] Y. K. Lee, J. Deval, P. Tabeling, and C. M. Ho, *Proc. MEMS2001*, 483, Interlaken, 2001.
[10] D. D'Alessandro, M. Dahleh, and I. Mezic, IEEE Trans. Autom. Control **44**, 1852 (1999).
[11] M. Volpert, I. Mezic, C. Meinhart, and M. Dahleh, *Proc. ASME Mech. Eng. Int. Congress and Exposition*, Nashville, TN, 1999, p. 483.
[12] M. Ottino, *The Kinematics of Mixing, Stretching, Chaos and Transport* (Cambridge University Press, Cambridge, England, 1989).
[13] X. Niu and Y. K. Lee, J. Micromech. Microeng. **13**, 452 (2003).
[14] M. Unger, H. Chou, T. Thorsen, A. Scherer, and S. Quake, Science **288**, 113 (2000).
[15] B. H. Weigl and P. Yager, Science **283**, 346 (1999).